Metadata of the chapter that will be visualized in SpringerLink

Book Title	Light Metals 2023	
Series Title		
Chapter Title	Heavy Metal Emissions Through Particulate Matter from Aluminium Electrolysis	
Copyright Year	2023	
Copyright HolderName	The Minerals, Metals & Materials Society	
Author	Family Name	**Müller**
	Particle	
	Given Name	**Fride**
	Prefix	
	Suffix	
	Role	
	Division	Department of Materials Science and Engineering
	Organization	Norwegian University of Science and Technology (NTNU)
	Address	Trondheim, Norway
	Email	
Author	Family Name	**Aarhaug**
	Particle	
	Given Name	**Thor Anders**
	Prefix	
	Suffix	
	Role	
	Division	
	Organization	SINTEF Industry
	Address	Trondheim, Norway
	Email	
Corresponding Author	Family Name	**Tranell**
	Particle	
	Given Name	**Gabriella**
	Prefix	
	Suffix	
	Role	
	Division	Department of Materials Science and Engineering
	Organization	Norwegian University of Science and Technology (NTNU)
	Address	Trondheim, Norway
	Email	gabriella.tranell@ntnu.no

Abstract

Heavy metal emissions from the aluminium industry are mainly carried from the plant through fugitive particulate matter (PM) originating from the aluminium electrolysis pot room. To evaluate the behaviour of metal-carrying PM, both airborne and settled PM from two different primary aluminium smelters have been characterized and analyzed for composition and particle size distribution, with special emphasis on heavy metals and carbon. In addition, optical particle sensors have been placed at different elevations in one of the plants to determine the concentrations of different particle sizes in fugitive PM. Metals such as

Fe and Ni were primarily found as particles together with S and P on partly combusted carbon PM. Settled PM from both plants were generally coarser (mean = 32–39 μm) and had a higher Al:Na ratio compared with airborne PM, with a mean PM of 21–22 μm. The optical sensors measured PM100 concentrations at roof level in the plant 5–6 times higher than the PM10 concentration during fuming events such as anode shift operations.

Keywords (separated by '-')	Aluminum - Heavy metals - Fugitive emissions - Particulate matter

Layout: T3 Grey | Book ID: 540883_1_En | Book ISBN: 978-3-031-22531-4
Chapter No.: 89 | Date: 28-11-2022 | Time: 12:29 pm | Page: 1/10

Heavy Metal Emissions Through Particulate Matter from Aluminium Electrolysis

Fride Müller, Thor Anders Aarhaug, and Gabriella Tranell

Abstract

Heavy metal emissions from the aluminium industry are mainly carried from the plant through fugitive particulate matter (PM) originating from the aluminium electrolysis pot room. To evaluate the behaviour of metal-carrying PM, both airborne and settled PM from two different primary aluminium smelters have been characterized and analyzed for composition and particle size distribution, with special emphasis on heavy metals and carbon. In addition, optical particle sensors have been placed at different elevations in one of the plants to determine the concentrations of different particle sizes in fugitive PM. Metals such as Fe and Ni were primarily found as particles together with S and P on partly combusted carbon PM. Settled PM from both plants were generally coarser (mean = 32–39 µm) and had a higher Al:Na ratio compared with airborne PM, with a mean PM of 21–22 µm. The optical sensors measured PM100 concentrations at roof level in the plant 5–6 times higher than the PM10 concentration during fuming events such as anode shift operations.

Keywords

Aluminum • Heavy metals • Fugitive emissions • Particulate matter

Introduction

Through international agreements, the primary aluminium industry has, together with other industries, committed to reducing greenhouse gases, as well as managing and monitoring hazardous waste and emissions of heavy metals in relation to their processes. In Norway, a significant fraction of certain reported heavy metal emissions from the land-based industries originates from aluminium production, as summarised in Table 1. These heavy metal emissions are mainly carried from the plant through fugitive particulate matter (PM) from the pot room with electrolysis cells and calculated based on regular measurements using PM collection filters over a period of weeks, with a known air throughput [1]. The PM typically originates from daily operational processes such as anode change, anode covering processes and metal tapping.

The heavy metals are primarily introduced to the electrolysis process through the carbon anodes and will distribute between metal (main path), bath and air/dust [3]. Carbon anodes are typically made of a mixture of 60–70% calcined petroleum coke (CPC), 15–20% recycled anode butts, and 12–17% coal tar pitch binder. The CPCs may contain different amounts of impurities, such as heavy metals, due to mixing different quality cokes [4]. In Table 2, some of the reported trace elements found in anode coke and their associated concentrations are given. In comparison, the metal content of the alumina raw materials is significantly lower than that of the coke [5].

As seen from Table 2, sulfur is a major impurity in the anode coke. The sulfur can be found as a part of the carbon lattice, attached to chains on the surface of clustered molecules or on surfaces and pores bound by capillary condensation, adsorption, or chemisorption [6]. A recent study [7] showed that V, Ni, and Fe are most likely present in high-sulfur coke mainly as hexagonal sulfides: V was found mainly as V_3S_4, Ni as hexagonal NiS and Fe as hexagonal FeS. These authors found that the metal was well distributed

F. Müller · G. Tranell (✉)
Department of Materials Science and Engineering, Norwegian University of Science and Technology (NTNU), Trondheim, Norway
e-mail: gabriella.tranell@ntnu.no

T. A. Aarhaug
SINTEF Industry, Trondheim, Norway

S. Broek (ed.), *Light Metals 2023*, The Minerals, Metals & Materials Series,
https://doi.org/10.1007/978-3-031-22532-1_89

Layout: T3 Grey | Book ID: 540883_1_En | Book ISBN: 978-3-031-22531-4
Chapter No.: 89 | Date: 28-11-2022 | Time: 12:29 pm | Page: 2/10

Table 1 Reported Norwegian heavy metal emissions from land-based industries and emissions from primary aluminium production in 2020 (kg) [2]

Element	Emission all land-based industries (kg/y)	Emission aluminium industry (kg/y)	Percentage emission from Al industry
Ni	10,143	2880	28
Pb	2410	260	11
V	733	96	13
Cd	141	26	19
Zn	22,158	898	4

Table 2 Representative concentration of trace elements in anode coke (ppm) [5]

Element	Low	High
Fe	50	350
Ni	50	500
V	30	500
Cu	20	50
Cr	1	50
P	5	30
Pb	3	10
S (wt%)	0.5	5
Mo	10	20
Na	20	140
Al	20	250
K	10	20
Zn	2	150
Mg	50	200

in the carbon matrix and not present as large crystalline inclusions. Previous studies of collected PM in potrooms [8, 9] have found it to consist of bath related compounds (cryolite, chiolite ($Na_5Al_3F_{14}$) and calcium chiolite ($Na_2Ca_3Al_2F_{14}$)), aluminas (γ-, γ'-, θ-, and α-Al_2O_3) and graphitic carbon with metallic and light metal impurities. Reported concentrations of heavy metal (oxides) in these dusts were in the order of 0.2–3.2%. Pot fumes are reported to be mainly fine particles with at least 50% of the particles <20 μm [10] in size. This corresponds with prior extensive studies of PM from electrolysis raw gas [11].

While previous studies have provided information on typical compositions and particle sizes of potroom PM, a more complete picture of the presence of heavy metals (chemical form, in which particle size bracket, coupling to operational events, etc.) in the fugitive PM emissions is needed to predict, for example, the metal-carrying particle dispersion in air from the plant. Hence, in the current work, the composition and particle size distribution of settled and airborne PM collected in electrolysis halls of two aluminium plants (denoted Plant A and Plant B), have been analysed. Special emphasis has been placed on the relationship between heavy metals and carbon in these materials. In addition, small, inexpensive optical sensors monitoring the in situ concentration of PM emissions were placed at different elevations in the potroom of Plant B to measure the relative concentrations of particle sizes and relate these to operational events. These sensors have previously shown promise in collecting useful data in the primary aluminium industry [12]. Put together, this data will provide a more "dynamic" understanding of metal emissions and thereby a better starting point for metal-containing PM dispersion estimates and modelling.

Experimental Procedure

Sampling of PM for Characterization

For both plants, PM deposited on the mezzanine floor above the electrolysis cell rows were collected by simply filling sample bottles, and denoted "settled". In Plant A, an "airborne" PM sample was collected over a 3-week period on a 50 mm filter in a probe connected to a vacuum pump placed at the regular sampling point at one of the gas ventilation points of the pot room. In Plant B, two airborne PM samples were collected through gas vacuum pumps fitted with 150 mm Whatman filters and neoprene hose and probe. Each sample was collected over a 3-week period: one above the mezzanine floor close to the roof opening (see sketch in Fig. 1) and the second, placed on a frame near floor level.

Collected PM Characterization

Imaging/Individual Particle Analysis

The collected PM was imaged using a Zeiss ULTRA 55 scanning electron microscope (SEM) with a field emission gun (FEG) and chemical composition analyses was done by means of energy dispersive spectroscopy (EDS). The PM was placed on carbon tape and additionally coated with carbon to give the best possible images and element analyses. The primary electron energy was set to 15 keV with a working distance (WD) of 10–15 mm. Individual sizes of carbon particles in the PM were additionally determined in selected samples via image analysis software in the SEM. For these measurements, PM was placed on copper tape rather than carbon tape.

Layout: T3 Grey | Book ID: 540883_1_En | Book ISBN: 978-3-031-22531-4
Chapter No.: 89 | Date: 28-11-2022 | Time: 12:29 pm | Page: 3/10

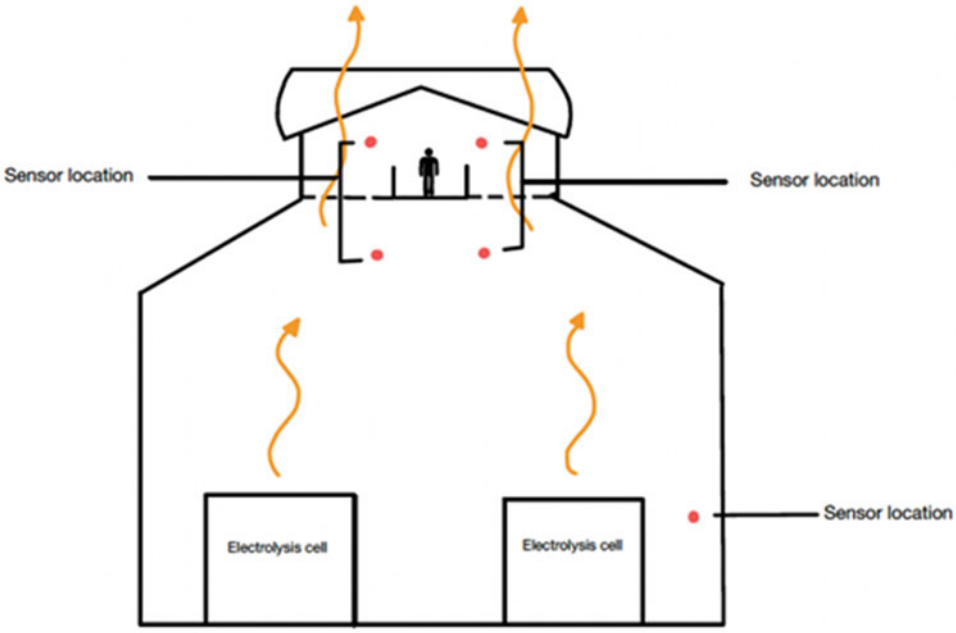

Fig. 1 Schematic of sensor location placements in Plant B

Particle Size

For all collected samples, at least three parallel particle size distribution analyses were carried out using a Horiba LA-960 laser scattering particle size distribution analyser, operating over a particle size range of 0.1–5000 μm. The analyser was operated in dry mode to be able to measure the size of the full sample, including water-soluble particles.

PM Composition

Full dissolution and subsequent Inductively Coupled Plasma–Mass Spectroscopy (ICP-MS) analysis of an airborne and a settled sample from Plant A was carried out by ALS Scandinavia in Sweden to determine the Al:Na ratio in the samples. The compositions of all collected samples, with emphasis on metals, P and S were analysed by Elkem Technology where two parallel samples were dissolved in an HNO_3-HCl-HF solution and analysed by Inductively Coupled Plasma-Optical Emission Spectroscopy (ICP-OES). It should be mentioned that the method did leave a fraction of the sample undissolved which leaves some uncertainty in the measurements. However, the reported concentrations were based on the original sample weight and hence, reported values would potentially be under-estimating rather than over-estimating concentrations. Additionally, the carbon content of the samples was determined by LECO with SINTEF Industry.

In Situ Measurements of Fugitive Dust Emissions

A set of Sensirion SPS30 optical PM sensors were used to gather in-situ data on mass and number concentrations of $PM_{1.0}$, $PM_{2.5}$, PM_4, and PM_{10} at three different locations/elevations in Plant B. Additionally, Nova SDS198 PM100 sensors were placed in the same locations to cover a wider particle size range. One of the sensor systems was placed at floor level, while the other two were placed at roof level near the rooftop outlet and hanging down over the cell rows, respectively. The sensor locations are illustrated in Fig. 1. Temperature and relative humidity were monitored simultaneously. For each location, three parallel sensors were connected to a small "Raspberry pi" computer, collecting data which can be accessed by an external computer, giving continuous measurements.

Results and Discussion

PM Imaging

In Fig. 2, typical images of PM from airborne and settled PM from Plant A are shown. As described by earlier studies, pot room PM consists of a mixture of condensed bath, alumina particles and carbon particles. As depicted in Fig. 3, a closer examination of the PM reveals that heavy metals largely appear as small inclusion clusters on partly combusted carbon particle surfaces.

Another example particle is displayed in Figs. 4a and b where Fe and Ni are observed on the carbon surface by use of Backscattered Electron (BSE) imaging, revealing their typical co-existence with S. The presence of Ni and Fe together with S is aligned with the observations by Jahrsengene [7] of the presence of Ni- and Fe-sulfides in anode coke, confirming that the carbon particles in fugitive PM relate to dusting from the carbon anodes.

Layout: T3 Grey | Book ID: 540883_1_En | Book ISBN: 978-3-031-22531-4
Chapter No.: 89 | Date: 28-11-2022 | Time: 12:29 pm | Page: 4/10

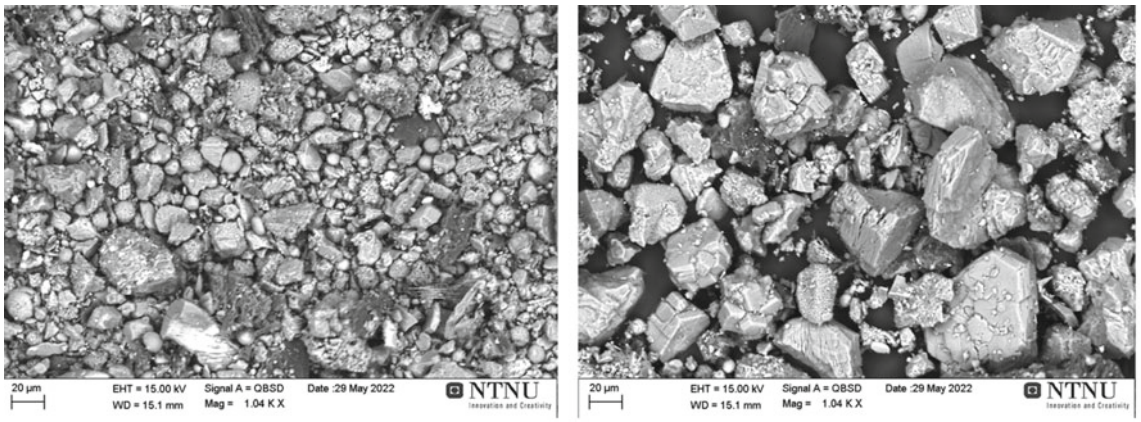

Fig. 2 Depiction of airborne (left) and settled (right) PM from Plant A as imaged through secondary electrons in SEM using identical magnification (X1000). The pictures illustrate clearly the difference in particle size between the two types of dust. At the chosen magnification, heavy metal particles can not be clearly distinguished

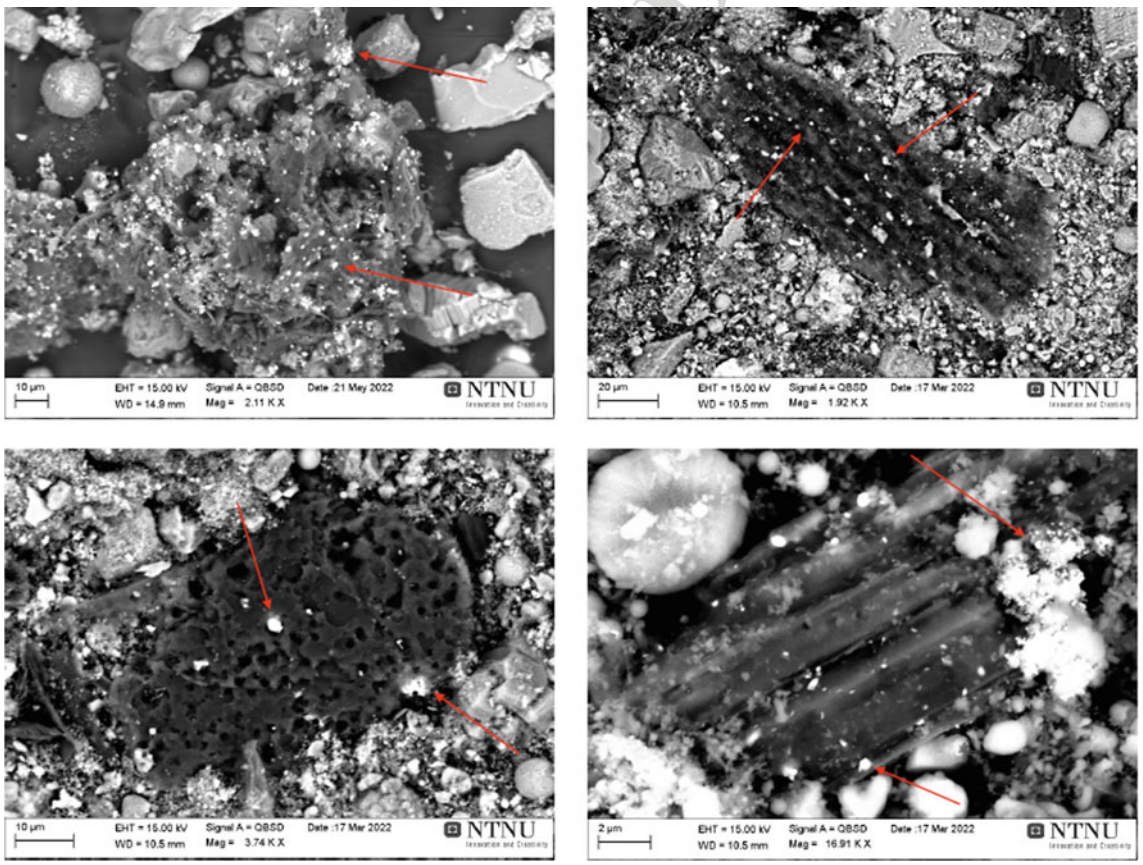

Fig. 3 Typical images of carbon particles in PM. Red arrows mark heavy metal particles

Similar elemental mapping of PM from electrolysis raw gas has also identified the co-existence of Ni and P [13], which corresponds well with a study performed by Haugland et al. [14] where the behaviour of phosphorus impurities in aluminium electrolysis cells were studied. These authors found that dissolved P species can also be reduced by impurities in the bath, where small carbon particles may act as nucleation sites. They also found that loss of phosphorous from the cell was due to evaporation of gaseous elemental phosphorous and that the phosphorus is attached to carbon dust.

Layout: T3 Grey | Book ID: 540883_1_En | Book ISBN: 978-3-031-22531-4
Chapter No.: 89 | Date: 28-11-2022 | Time: 12:29 pm | Page: 5/10

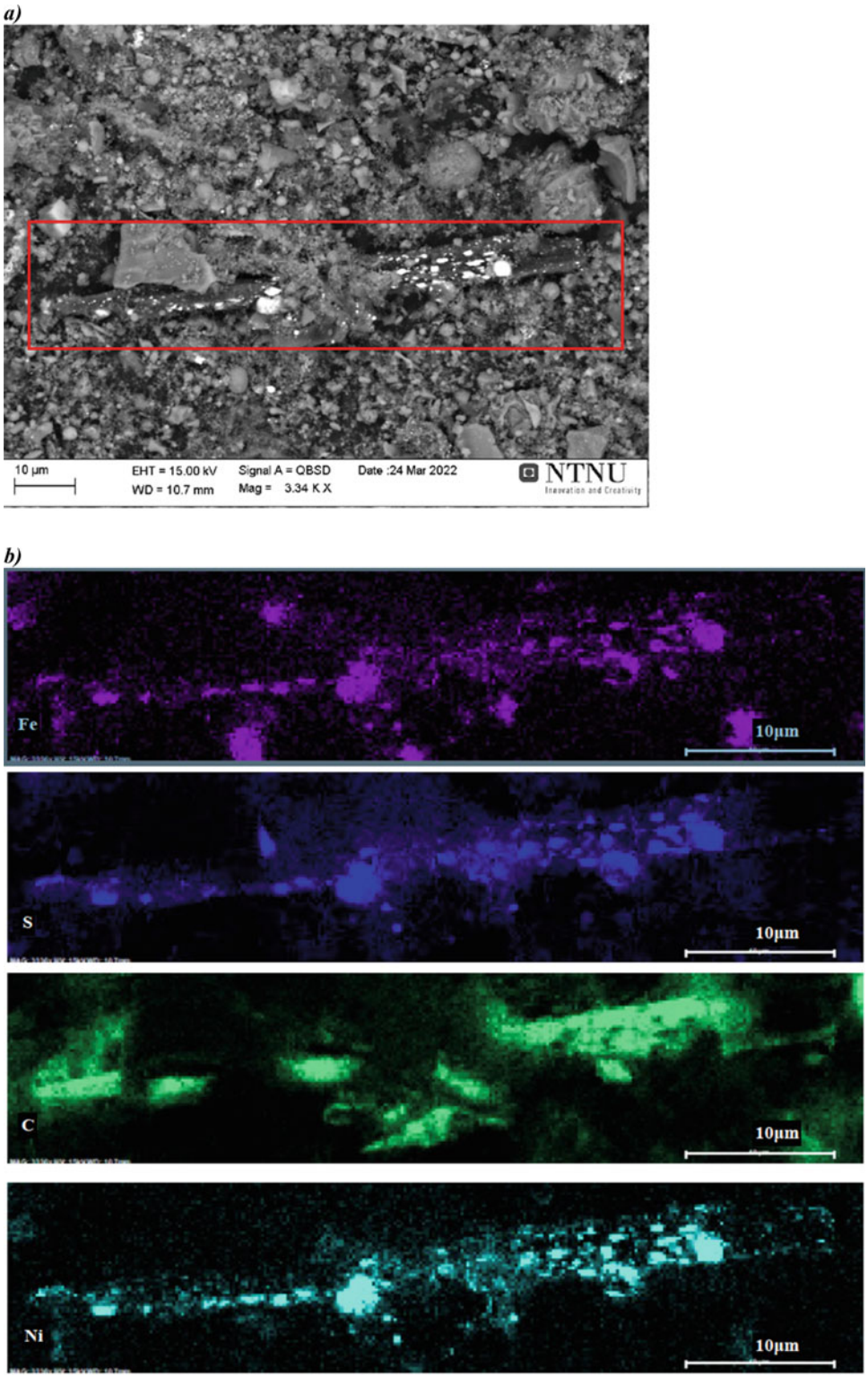

Fig. 4 **a** Secondary electron SEM image of a carbon particle in a matrix of alumina and bath fume. **b** Backscattered electron imaging of the carbon particle in **a** illustrating the composition of the bright spots on the carbon surface

Layout: T3 Grey | Book ID: 540883_1_En | Book ISBN: 978-3-031-22531-4
Chapter No.: 89 | Date: 28-11-2022 | Time: 12:29 pm | Page: 6/10

Particle Size

Figure 2 is a visual illustration of the difference in particle size appearance between airborne and settled PM from Plant A. Laser scattering measurements confirm the visual observations as detailed by the particle size distribution curves for different airborne and settled samples from both Plant A and B in Fig. 5. The collected particle size data is summarized in Table 3, showing that the mean particle size of settled PM lies between approximately 32–39 µm, while the mean particle size of airborne PM lies between 21 and 22 µm. Interestingly, when manually measuring the size in the SEM of 100 randomly selected carbon particles in airborne and settled PM, respectively (Fig. 6), the mean size of these particles came out almost double the size of the measured mean of all particles using laser diffraction [15]. While this difference may reflect a selection bias of particles measured manually, it is possible that carbon particles in fugitive emissions are generally larger and more buoyant than other, higher density particles, such as alumina, and consequently preferentially report to the gas escaping the plant.

Particle Composition

The Al concentration of settled PM from Plant A was measured to 72.4% while that of airborne PM was on average 59.6%. However, the Na content was higher in the airborne PM (30.7%) than the settled PM (21.9%). This indicates a higher concentration of bath fumes in the airborne PM and a higher concentration of alumina in the settled PM, which is rather expected. In Table 4, selected metallic, P, S, and C contents of the settled and airborne samples from the two plants are summarized.

Two main trends can be observed in Table 4. The first is that both the metal and light element contents are on average slightly higher in the airborne than in settled PM samples. Since the metal content appears to be mostly associated with carbon particles, this is a logical outcome. However, the compositional uncertainty in the carbon content makes this difference statistically insignificant. The composition of airborne PM from roof and floor level, respectively, in Plant B are not significantly different. The second trend is that both metal, carbon and phosphorous contents are higher

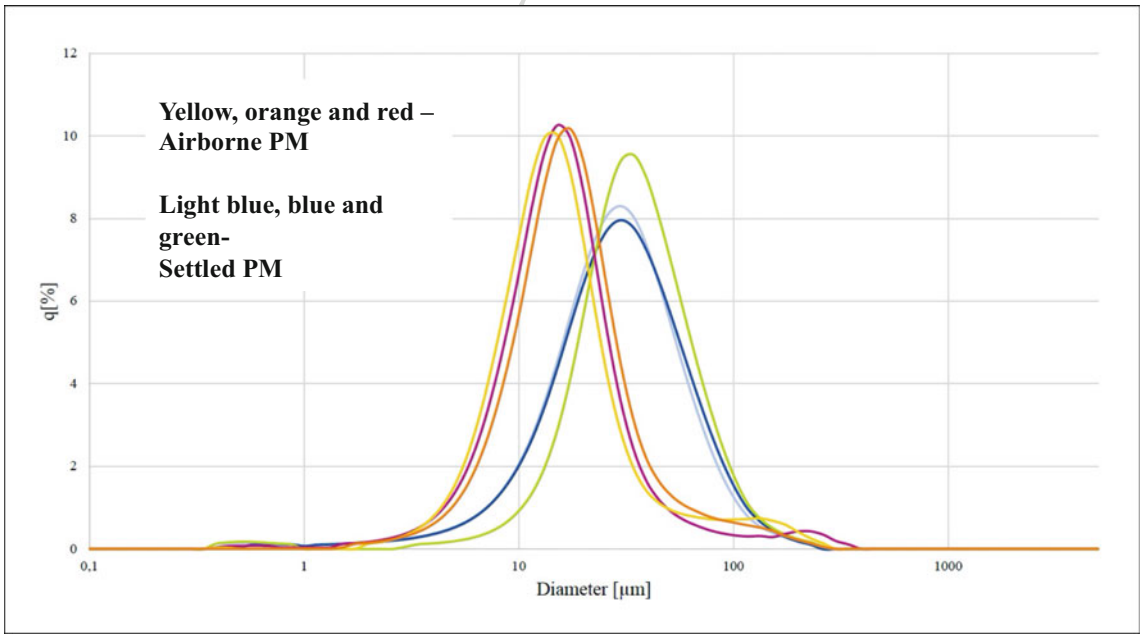

Fig. 5 Particle size distribution of airborne and settled PM samples

Table 3 Particle size distribution for airborne and settled PM (µm)

Particle size (µm)	Airborne			Settled		
	A-1	A-2	A-3	A-1	A-2	B-1
Median	14.3	13.6	15.7	26.6	27.4	31.9
Mean	21.4	21.7	21.9	32.8	34.1	38.6
D_{10}	6.63	6.57	7.37	10.0	10.1	11.0
D_{90}	47.3	46.0	38.4	61.9	65.6	49.4

Layout: T3 Grey | Book ID: 540883_1_En | Book ISBN: 978-3-031-22531-4
Chapter No.: 89 | Date: 28-11-2022 | Time: 12:29 pm | Page: 7/10

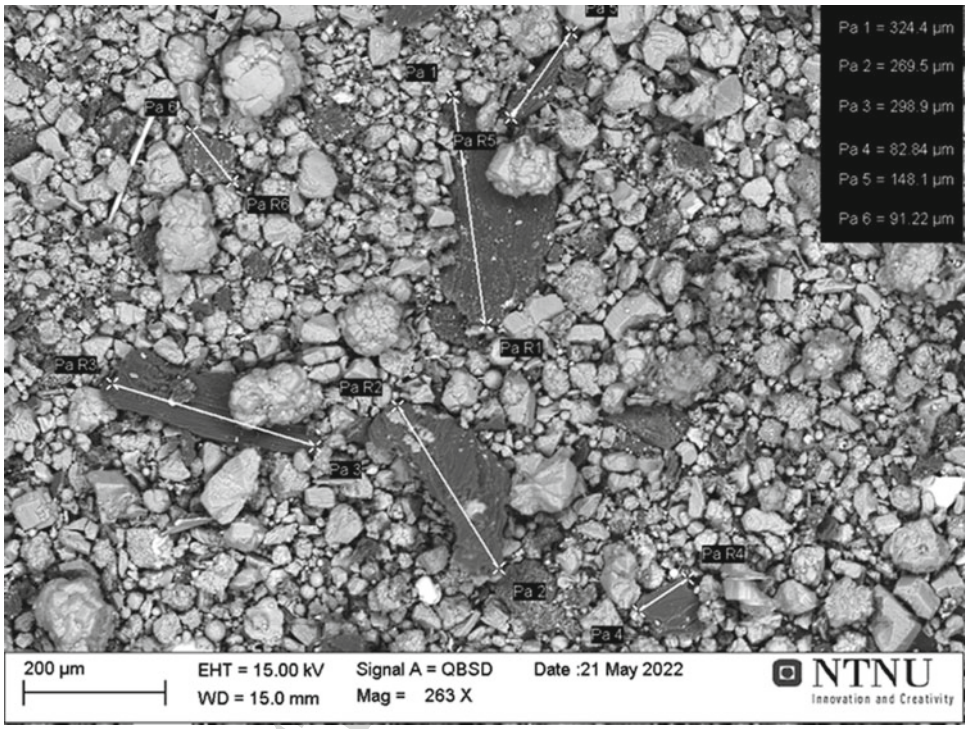

Fig. 6 Illustration of carbon particle measurements in a settled PM sample from Plant A using SEM imaging

Table 4 Selected metal, P and S contents of settled and airborne PM samples [µg/kg] as measured by ICP-OES. Wt% (C) measured by LECO. All ICP samples except airborne floor PM from Plant B (very little sample) were analyzed in two parallels. The reported variation is that between the two reported parallels. The LECO analysis for airborne PM in Plant B had no parallel

Element	Plant A		Plant B		
	Settled	Airborne	Settled	Airborne (roof)	Airborne (floor)
Fe	3500±0	6100±100	1700±0	2450±150	3400
Ni	3600±100	3550±50	1700±0	3000±200	2900
V	188±2	203±3	84±1	154±66	171
Pb	48±4	116±4	38±2	457±10	216
Mo	39±3	29±4	9±0	10±8	<10
S	3750±50	5100±600	3150±50	9650±350	8000
P	477±16	857±160	225±0	434±122	452
C (wt%)	9.5±1.4	9.8±1.2	7.07±0.7	7.3	8.2

in PM from Plant A than Plant B. The differing amount of carbon in the plant-specific PMs would likely be explained by operational reasons or the use of different carbon materials with different behavior in terms PM generation. The higher S content in airborne PM from Plant B than that in other PM samples is internally consistent with respect to settled PM but not consistent with respect to the lower C content than Plant A and its origin should hence be further investigated.

Particle Sensor Measurements

Figure 7 illustrates the online measurements of the PM10 particle sensor at roof level over a 10-day-long measurement period. It can be seen from the figure that regular "events" account for the bulk of PM emission with spikes reaching concentrations up to 2500 µg/m^3. These events coincide with anode shifts, allowing bath evaporation and carbon dust to leave the cell house as has previously been reported in the work of Wong [16] and Myklebust et al. [12].

While the PM 10 concentrations were similar at roof and cell levels, the floor-level PM10 concentrations are generally significantly lower than those above the cells and at roof level, as shown in Fig. 8.

In Table 5, the average mass concentrations of the different particle size bins are summarised. It is found that PM1.0 amounts to 86% of PM10 at roof level, while at floor level, the same fraction amounts to 77% of PM10. PM2.5 amounts to 95% of PM10 at roof level and 89% of PM10 at

Layout: T3 Grey | Book ID: 540883_1_En | Book ISBN: 978-3-031-22531-4
Chapter No.: 89 | Date: 28-11-2022 | Time: 12:29 pm | Page: 8/10

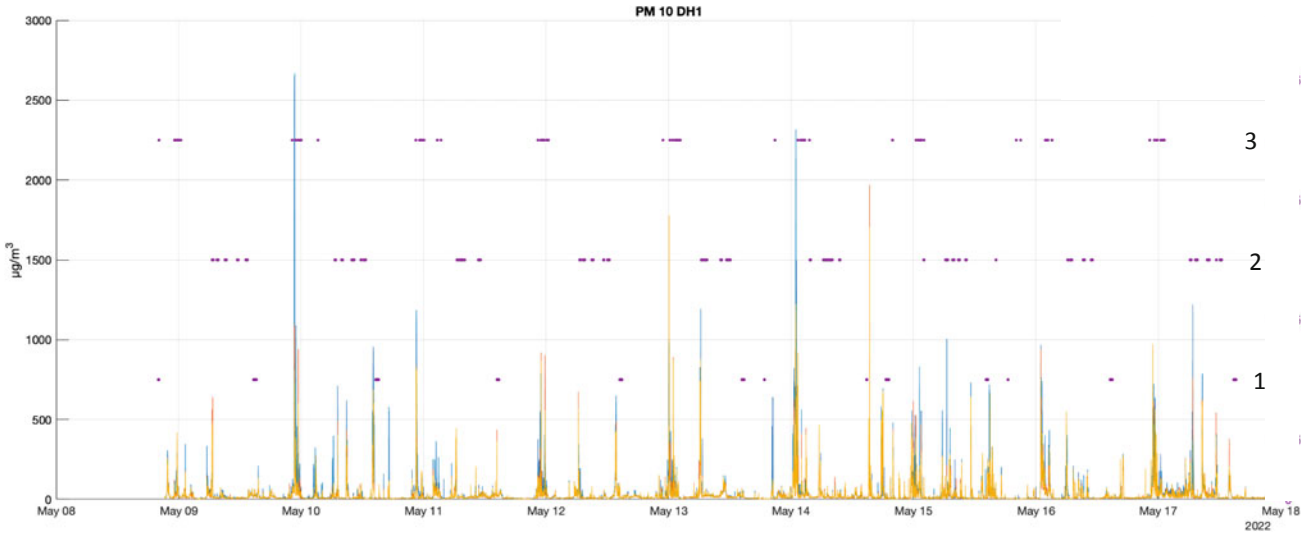

Fig. 7 PM concentration of the 3 parallel PM 10 sensors at roof level (different colored signals). Production activities marked on lines 1 = temperature measurements, 2 = tapping and 3 = anode change

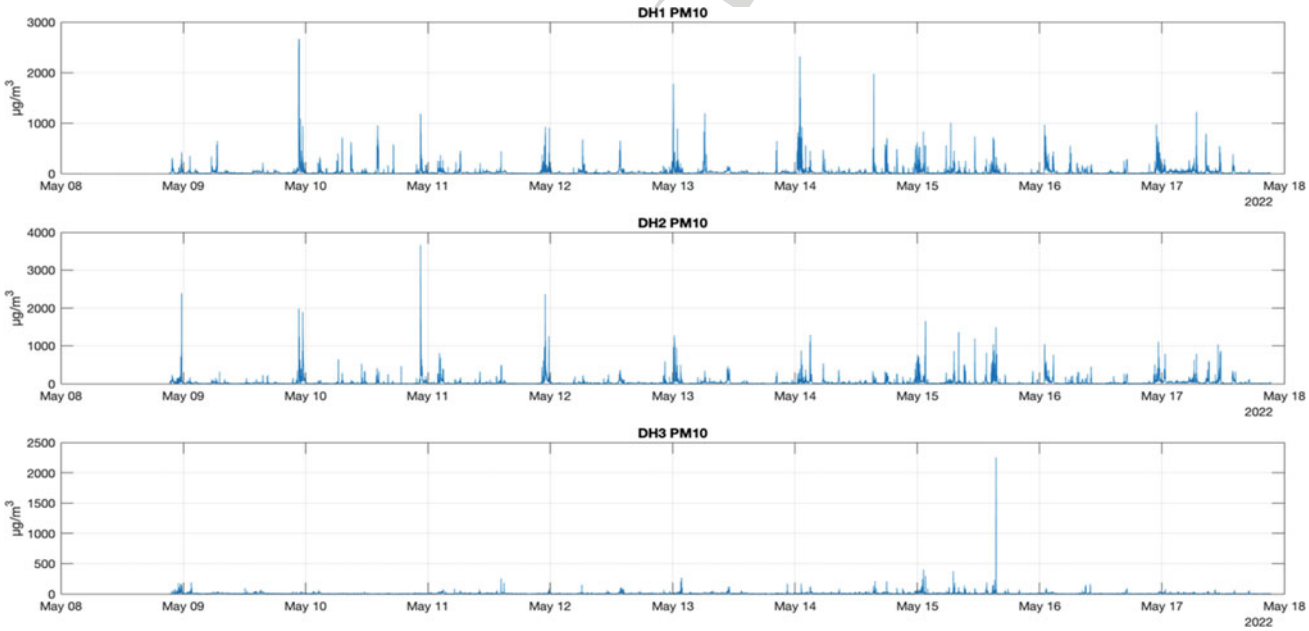

Fig. 8 From the top: PM10 measured at (DH1) roof level, (DH2) cell level and (DH3) floor level

Table 5 Average PM mass concentrations for the low particle size (10PM) sensors in roof, over cell, and floor positions at Plant B

Av. mass concentration (µg/m^3)	Roof	Over cell	Floor
PM_1	26.4	29.6	6.7
$PM_{2.5}$	29.1	32.6	7.9
PM_4	30.1	33.7	8.5
PM_{10}	30.6	34.2	8.8

Layout: T3 Grey | Book ID: 540883_1_En | Book ISBN: 978-3-031-22531-4
Chapter No.: 89 | Date: 28-11-2022 | Time: 12:29 pm | Page: 9/10

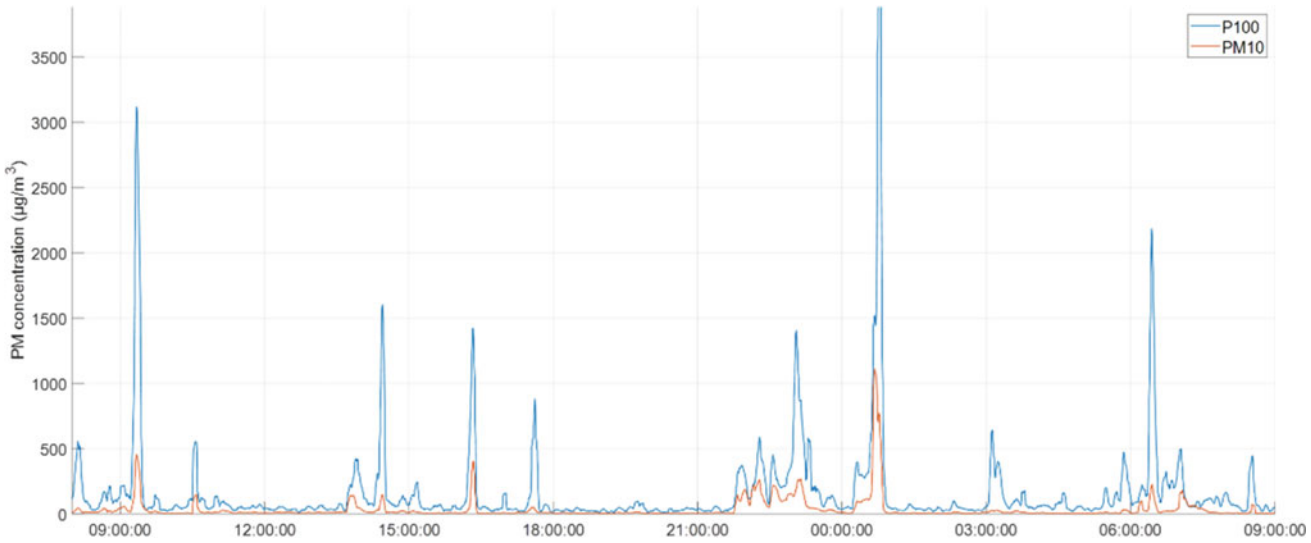

Fig. 9 Comparison of PM10 and PM100 concentration at roof level in Plant B over a 24 h period

floor level. Lastly, PM4.0 amounts to 98% and 96% of PM10 at roof and floor levels, respectively.

The PM10 sensors are rated to reliably measure a maximum of 1000 µg/m^3 while typically reporting up to 2500 µg/m^3 and are often "saturated" during process events. Given the particle size distribution measurements of collected PM in Fig. 5 and Table 3, PM100 sensors measuring at roof and floor levels were used to monitor the concentration of larger particles. These sensors are rated to a concentration up to 20.000 µg/m^3. A comparison between the PM10 and PM 100 measured at roof level is illustrated in Fig. 9. As seen in the figure, the measured concentration ratio between PM100 and PM10 during major events is between 5 and 6. This is in line with the measured particle size distribution of the collected PM samples. The relative background PM concentrations measured by the two different sensor types may, however, be somewhat different. Therefore, one should be careful when comparing measured absolute PM100 and PM10 concentrations.

Conclusions

Airborne and settled PM from two different primary aluminium smelters (Plants A and B) have been characterized and analyzed for composition and particle size distribution with special emphasis on heavy metals and carbon. In addition, optical particle sensors have been placed at different elevations in Plant B to determine the concentrations of different particle sizes in fugitive PM. The following conclusions are drawn:

- Both settled and airborne PM generally consists of bath fume, alumina particles, and carbon particles.
- Heavy metals such as Fe and Ni are largely coexisting with S on the surface of partly combusted carbon particles.
- The S, P and heavy metal contents are on average slightly higher in airborne than in settled PM for both plants. The Na content is higher while the Al content lower in the airborne PM, indicating a higher bath content and a lower alumina content in the airborne PM.
- The heavy metal content, C and P content is higher in PM from Plant A than B but the S content lower.
- Settled PM in both plants were generally coarser that airborne PM with a mean PM measured by laser scattering, lying between approximately 32–39 µm for settled PM while the mean particle size of airborne PM was measured between 21 and 22 µm. Carbon particles were typically larger than other dust particles.
- High particle concentrations (>1000 µg/m^3) were measured by the optical sensors during anode shift at the roof level of Plant B. The mean PM10 particle concentration over the 10-day period for the roof level and over the electrolysis cells were between 30 and 40 µg/m^3, while that at floor level was close to 6–9 µg/m^3. PM1 accounted for 77–86% of the measured PM10. The measured PM100 concentration was between 5 and 6 times higher than the PM10 concentration during fuming events at roof level.

Layout: T3 Grey | Book ID: 540883_1_En | Book ISBN: 978-3-031-22531-4
Chapter No.: 89 | Date: 28-11-2022 | Time: 12:29 pm | Page: 10/10

Future Work

As a continuation of the current work, a three-stage impactor will be used in both Plant A and B over an extended period of time in order to collect and measure PM online. This will allow for more specific correlation between composition analysis of different size fractions and their counts/masses. Calibration of different particle sensor "background" concentration measurements should be performed in order for a more reliable comparison between intensities.

Acknowledgements This publication has been funded by the SFI Metal Production (Centre for Research-based Innovation, 237738). The authors gratefully acknowledge the financial support from the Research Council of Norway and the partners of the SFI Metal Production. The authors also wish to thank Ole Kjos at SINTEF industry for aiding the placement of PM100 sensors in Plant B.

References

1. Norwegian standards NS 4861 and NS 4863.
2. Miljødirektoratet og Statistisk Sentralbyråd. Landbasert industri, 2022. Accessed: 28.04.2022. [Online]. Available: https://www.norskeutslipp.no/no/Landbasert-industri/?SectorID=600.
3. G. Jahrsengene, H. C. Wells, A. P. Rørvik, S.and Ratvik, R. G. Haverkamp, and A. M. Svensson. "A XANES study of sulfur speciation and reactivity in cokes for anodes used in aluminium production", Metallurgical and Materials Transactions B, volume 49, pages 1434–1443. 2018.
4. L. Edwards, N. Backhouse, H. Darmstadt, and M. Dion. "Evolution of anode grade coke quality", Light Metals, pages 1207–1212. 2012, Springer International Publishing.
5. T. A. Aarhaug and A. P. Ratvik, "Aluminium primary production off-gas composition and emissions: An overview", JOM, volume 71, pages 2966–2977. 2019.
6. G. Jahrsengene. "Coke impurity characterisation and electrochemical performance of carbon anodes for aluminium production", PhD Thesis, NTNU, ISBN: 9788232643004, 2019.
7. G. Jahrsengene, H. C. Wells, C. Sommerseth, A. P. Ratvik, L. P. Lossius, K. H. Sizeland, P. Kappen, A. M. Svensson, and R. G. Haverkamp "An EXAFS and XANES study of N, Ni, and Fe speciation in cokes for anodes used in aluminum production", Metallurgical and Materials Transactions B, volume 50, pages 2969–2981, 2019.
8. B. L. W. Höflich, S. Weinbruch, R. Theissmann, H. Gorzawski, M. Ebert, H. M. Ortner, A. Skogstad, D. G. Ellingsen, P. A. Drabløs, and Y. Thomassen. "Characterization of individual aerosol particles in workroom air of aluminium smelter potrooms", Journal of Environmental Monitoring, volume 7, pages 419–424, 2005, Royal Society of Chemistry.
9. D. S. Wong, N. I. Tjahyono, and M. M. Hyland "The nature of particles and fines in potroom dust", Light Metals, pages 553–558. 2014 Springer International Publishing.
10. M.M. Hyland and M.P. Taylor, "Origins and effects of potroom dust", Light Metals, pages 141–145. 2005, Springer International Publishing
11. H. Gaertner, "Characteristics of particulate emissions from aluminium electrolysis cells", PhD Thesis, 2013. NTNU, ISBN:978-82-471-4764-1.
12. H. A. H. O. Myklebust, T. A. Aarhaug, and G. Tranell, "Measurement system for fugitive emissions in primary aluminium electrolysis" Light Metals, pages 735–743, 2020, Springer International Publishing.
13. F. Müller, "Heavy metal emissions from primary aluminium production" Technical report, 2021. NTNU.
14. E. Haugland, G. M. Haarberg, E. Thisted, and J. Thonstad, "The behaviour of phosphorus impurities in aluminium electrolysis cells", Essential Readings in Light Metals: Volume 2 Aluminum Reduction Technology, pages 229–233, 2016, Springer International Publishing.
15. F. Müller, "Heavy metal emissions from primary aluminium production" MSc thesis 2022. NTNU.
16. D. S. Wong, M. M. Hyland, N. I. Tjahyono, and D. Cotton, "Potroom operations contributing to fugitive roof dust emissions from aluminium smelters" Light Metals, pages 905–912, 2019 Springer International Publishing.

Author Query Form

Book ID : **540883_1_En**

Chapter No : **89**

Please ensure you fill out your response to the queries raised below and return this form along with your corrections.

Dear Author,

During the process of typesetting your chapter, the following queries have arisen. Please check your typeset proof carefully against the queries listed below and mark the necessary changes either directly on the proof/online grid or in the 'Author's response' area provided below

Query Refs.	Details Required	Author's Response
AQ1	Please confirm if the section headings identified are correct.	
AQ2	The comma have been changed to a decimal point globally throughout this chapter. Please check and correct if necessary.	